Research Article

Journal of Environmental Nanotechnology

Characterization of MgO Cubic Nanocrystals Synthesized and Deposited on rGO Nanosheets

V. Shanmugam[1*], T. Seethalakshmi[1], M. Vishnu Devan[2] and T. Deepa[2]

[1]Department of Physics, Government Arts College, Affiliated to Bharathidasan University, Karur, TN, India
[2]Department of Chemistry, Government Arts College, Affiliated to Bharathidasan University, Karur, TN, India
Received: 09.08.2024 Accepted: 05.11.2024 Published: 30.03.2025
*nvsgacphy@gmail.com

ABSTRACT

The present study focuses on synthesizing rGO and MgO/rGO nanoparticles using Hummer's and co-precipitation methods. Using X-ray diffraction (XRD), High-resolution transmission electron microscopy (HR-TEM), Energy dispersive X-ray analysis (EDAX), Fourier transform infrared spectroscopy (FTIR), Ultraviolet-visible spectroscopy (UV-Vis), Photo-luminescence spectroscopy (PL), and Cyclic voltammetry (CV), the synthesized rGO and MgO/rGO nanoparticles were characterized structurally, morphologically, and optically. The XRD data revealed the cubic structure of the nanoparticles. The dislocation density value was 0.3185×10^{15} and the Debye-Scherrer formula determined the crystallite size as 56.0316 nm. According to UV data, the absorption peak was located at a wavelength of 267 nm, and the band gap value was 4.6441 eV. The vibration frequency parameters of MgO at 548 cm^{-1} were in good agreement with the published research. The elements in magnesium and oxygen were verified by Energy-dispersive X-ray analysis. The photoluminescence spectrum displayed green, blue, and violet emissions from rGO and MgO/rGO nanoparticles. For rGO and MgO/rGO nanoparticles, the specific capacitance values were determined to be 18 F/g and 51F/g, respectively.

Keywords: Specific capacitance; Nanoparticles; Dislocation density; Photo-luminescence; Band gap; XRD.

1. INTRODUCTION

In recent times, there has been a notable surge in scientific and technological interest in graphene oxide (GO), which is the precursor of graphene (Akrami *et al.* 2019). Because of its excellent mechanical strength and simplicity of functionalization, graphene oxide (GO) has found widespread applications (Bhargava *et al.* 2017). Because of its extraordinarily large specific surface area, abundance of oxygen-containing surface functions, and high water solubility, GO may also be the perfect platform for the immobilization of enzymes (Saini *et al.* 2016). Owing to these remarkable qualities, graphene finds extensive use in energy harvesting, photo-catalysis, optoelectronics, supercapacitors, sensors, nanocompo-sites, nano-electronics, batteries, and other fields (Saini *et al.* 2016).

There are numerous ways to reduce graphene oxide (GO), including chemical reduction using sodium bromide and hydrazine hydrate (Liu *et al.* 2015), laser irradiation (Sarkar *et al.* 2013), microwave irradiation (Zhang *et al.* 2015), photo-reduction (Sudesh *et al.* 2013), hydrothermal reduction (Wahab *et al.* 2018) and thermal reduction. Reduced graphene oxide (rGO) is the general term for the graphene product obtained using the aforementioned techniques. By altering the graphene sheet's edge structure and chemically modifying its interior or edges, the attached functional groups are eliminated during the reduction of graphene oxide (GO) to reduced graphene oxide (rGO). It is possible to modify the optical, magnetic, and electrical properties of GO by reducing it. Magnesium oxide nanoparticles have special properties that make them useful as fuel additives, refractory materials for coating filler, and a variety of electrical and high-temperature devices (Sun *et al.* 2016; Abdel-Aal *et al.* 2018).

Magnesium oxide (MgO) is a significant inorganic oxide that is widely applied in numerous fields. It is a semiconductor that crystallizes in a cubic form resembling rock salt or sodium chloride (Wang *et al.* 2018). MgO nanoparticles have been synthesized using a variety of synthesis techniques, including sol-gel, hydrothermal, flame spray pyrolysis, combustion, aqueous wet chemical, surfactant, and chemical gas phase deposition.

Additionally, a variety of physicochemical methods exist for creating nanoscale MgO particles. Numerous factors, including pH, ionic strength, precipitation temperature, and various calcination temperatures, can regulate the size and shape of oxide particles. Here in this study characterisation of reduced Graphene Oxide (rGO) and MgO nanoparticles deposited over rGO nanosheets have been studied and compared using UV-Vis and Photo luminescence spectroscopy.

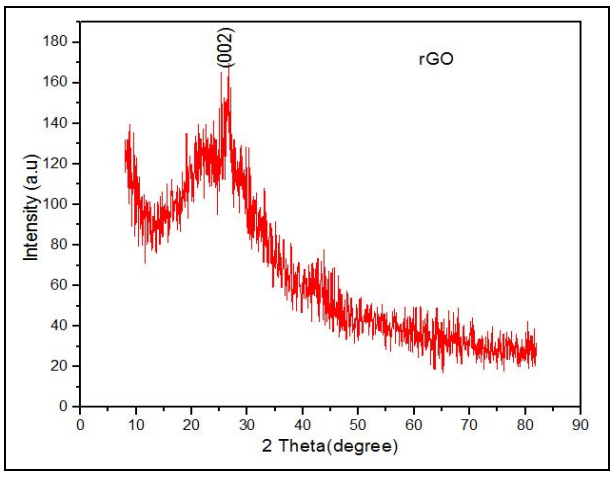

Fig. 1: XRD pattern of rGO nanoparticles

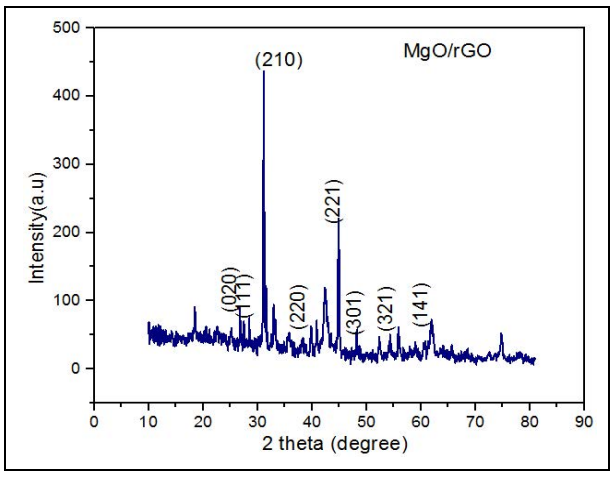

Fig. 2: XRD pattern of MgO/rGO nanoparticles

Table 1. XRD pattern of MgO/rGO nanoparticles

Sample	Pos. [° 2 Th.]	d-spacing [Å]	Crystallite size (nm) (D)	Micro-strain (10^{-3} m) (ε)	Dislocation density (10^{15}) (L/m^2)
rGO	26.5845	2.1098	50.3157	0.7393	0.3949
MgO/rGO	31.1593	2.8704	56.0316	2.3027	0.3185

2. EXPERIMENTAL PROCEDURE

2.1 Synthesis of Graphene Oxide (GO)

In the current work, GO was synthesized using a modified version of the Hummer process. A predetermined amount of 2.5 g of graphite powder was mixed with 70 ml of H_2SO_4 in a 500 ml beaker. After adding 7 g of $KMnO_4$ progressively, the mixture was agitated for 3 h in an ice bath. After that, the mixture was gradually stirred for an hour while 200 ml of distilled water was added. To produce a light-yellow suspension, 30 ml of H_2O_2 solution were added to finally stop the reaction. The final product was cleaned using distilled water and an aqueous solution containing 1% HCl. After the process was completed, the particles were kept in the oven and dried at 60 °C.

2.2 Synthesis of Reduced Graphene Oxide (rGO)

rGO was created using the prescribed procedure. 0.25 g of GO was dispersed in 50 ml of deionized water and ultrasonicated it for 45 minutes. Then the mixture was ultrasonically sonicated for one hour after a minor amount of $NaBH_4$ was added. After three rounds of washing with deionized water, the resultant rGO was dried at 60 °C in the oven.

2.3 Synthesis of MgO/rGO Nanoparticles

Co-precipitation was used for producing MgO/rGO nanoparticles. Sodium hydroxide (NaOH), sodium bromide ($NaBH_4$), and magnesium chloride ($MgCl_2.6H_2O$) were the starting ingredients employed in the synthesis. 0.40 g of magnesium chloride was added to 50 ml of DD water and thoroughly mixed for 15 minutes. After stirring for 30 minutes, 0.08 g of sodium hydroxide and 0.075 g of sodium bromide were added straight to the mixture mentioned above. At last, we add 0.3 g of rGO and stir continuously for 6 h. After being removed from the oven, the sample was dried. The final mixture is heated for 30 minutes.

3. RESULTS AND DISCUSSION

3.1 X-Ray Diffraction Studies (XRD)

Powder X-ray diffraction was used to analyze the crystal structure of the produced sample using Cu-Kα radiation (λ=0.15456 nm). The prepared samples' phase purity and crystal structure were assessed using an X-ray diffraction pattern, as illustrated in Fig. 1. In the 22–280 range, rGO exhibited a large diffraction peak (002). The rGO peaks can be mapped to the hexagonal structural planes by applying the formula [Xpert Pro High score (Ref. No. 00-033-1161) α=β≠ γ]. The produced MgO/rGO nanoparticles' X-ray diffraction is depicted in Fig. 2. The intervals (020), (111), (210), (220), (221), (301), (321), (141), and (232) can be used to index the diffraction peaks at 26.79°, 28.50°, 31.15°, 39.87°, 44.90°, 48.26°, 55.85°, 60.68°, and 65.75°. MgO/rGO nanoparticles' XRD pattern is compared to the JCPDS Data (00-005-0548). The MgO/rGO nanoparticle has a particle size of 55.90 nm. The computed XRD pattern has a d-spacing of 2.83013 Å, lattice parameter value of 12.4992 Å, and micro-strain value of 2.307 nm. The Debye-Scherrer formula was utilized to compute the crystalline size:

$$D = 0.9\lambda / \beta \cos\theta \text{ nm} \quad \ldots (1)$$

where, D - crystalline grain size (nm), λ – wavelength of X-rays (nm), β-line broadening of full width at half maximum (FWHM) in radians, and θ – Bragg's diffraction angle in degrees.

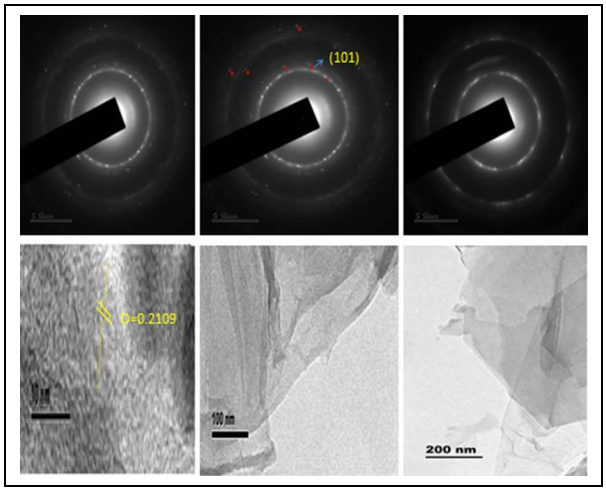

Fig. 3: TEM of rGO nanoparticles

3.2 Transmission Electron Microscopy (TEM)

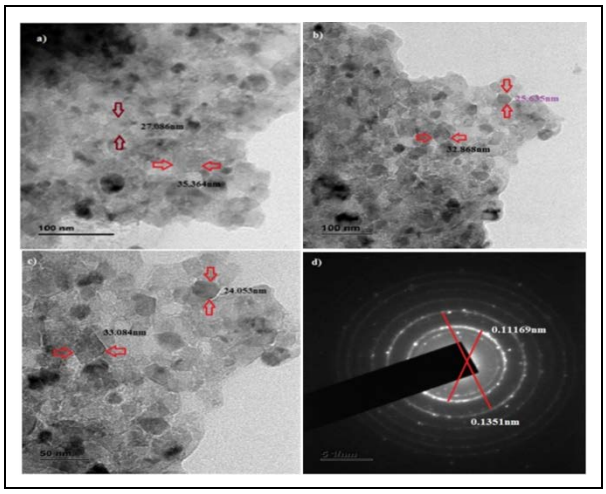

Fig. 4: (a, b, and c) TEM images and (d) SAED pattern of the MgO/rGO nanosheets

An electron transmission microscope (TEM) tool was used for visualizing and analyzing specimens from micro-space to nano-space. It makes it possible to examine crystal structures, specimen orientation, and chemical phase composition using X-ray and electron energy analysis, as well as diffraction patterns. Because of its ability to identify the location of atoms within materials, HR-TEM is a vital tool for studying nanotechnology. Fig. 3 illustrates the synthesized rGO's d-spacing value of 2.109 Å appropriately matches the rGO nanoparticles d-spacing value of 0.2109 nm within the HR-TEM result. It showed that there is a strong agreement between the d-spacing value of XRD and the d-spacing value of TEM. Fig. 3 shows the TEM image of MgO/rGO nanoparticles synthesized by hydrothermal method. The average particle size was 24.053 to 35.364 nm. Fig. 4(a, b, and c) shows that the MgO cubic nanocrystals were embedded on rGO nanosheet. TEM image confirmed the cubic nanocrystals. MgO/rGO nanoparticles were characterized by selected area electron diffraction (SAED), as shown in Fig. 4(d).

3.3 Energy Dispersive X-Ray Analysis (EDAX)

EDAX spectrum of MgO/rGO nanoparticles was subjected to EDAX analysis with the use of the tool energy dispersive X-ray Microanalyzer. The presence of elements in magnesium (Mg) and oxygen (O) were found in the EDAX spectrum, shown in Fig. 5.

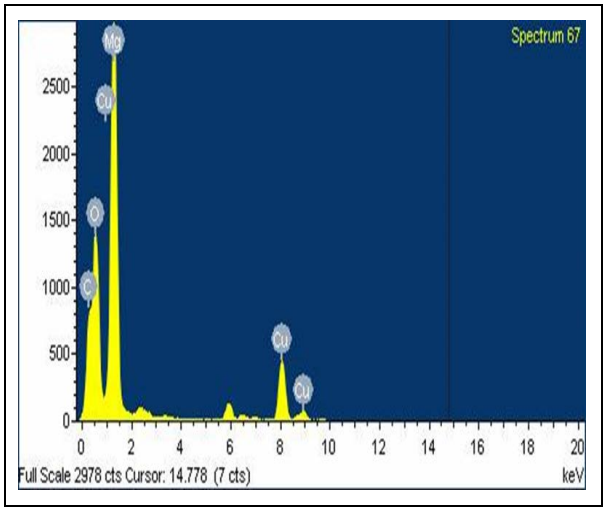

Fig. 5: EDAX image of MgO nanoparticles

Table 2. Elemental ratios in the MgO nanoparticles

Element	Weight %	Atomic %
C K	19.57	34.72
O K	18.33	24.41
Mg K	37.05	32.47
Cu K	25.05	8.40
Totals	100.00	

3.4 FT-IR Spectrum Analysis

The FT-IR spectrums were obtained in the 400–4000 cm^{-1} range using a Perkin–Elmer spectrum RXI Spectrometer and the KBr disk approach, as depicted in Fig. 6. Wavelengths above 3400 cm^{-1} were associated with an O-H stretching, and wavenumbers above 1570 cm^{-1} indicated the presence of functional groups such as O-C-O and C=C; this confirmed that there were few functional groups containing oxygen. Another new peak was found in the range of 1560 to 1581 cm^{-1}, which was related to the skeletal vibrations of unoxidized domains in the aromatic sections of graphene oxide (GO) or graphite.

Table 3. FTIR assignment of rGO and MgO/rGO nanoparticles

Wavenumber, cm^{-1}		Functional groups
rGO	MgO/rGO	
617	714	C=C bending
1109	1113	C-O Stretching
1581	1632	C=C Stretching
3446	3253	O-H Stretching

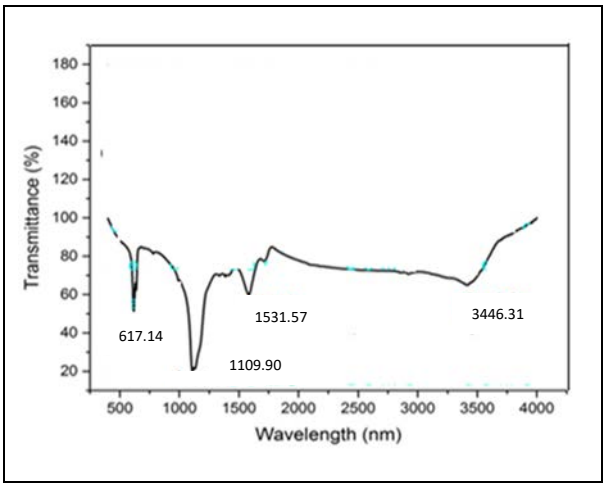

Fig. 6: FTIR spectrum analysis of rGO nanoparticles

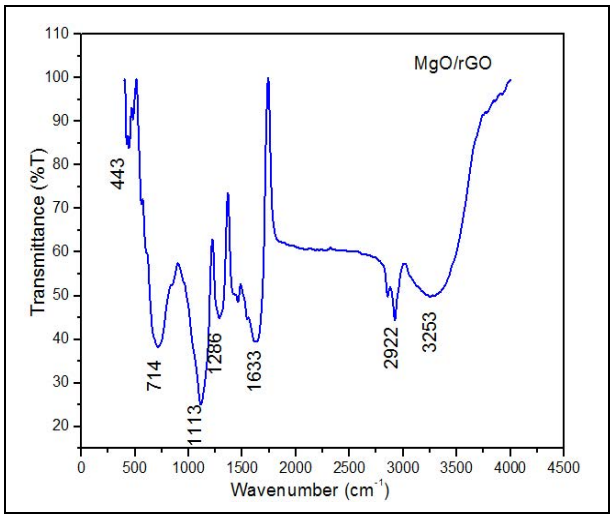

Fig. 7: FTIR spectrum analysis of MgO/rGO nanoparticles

Fig. 7 shows the FT-IR spectrum of synthesized MgO/RGO nanoparticles. The FT-IR spectra were recorded using a Perkin–Elmer Spectrum RXI Spectrometer with the KBr disk technique in the range of 400-4000 cm^{-1}. A strong and broad absorption peak at 3253 cm^{-1} was observed, which was due to O-H stretching vibrations. The small absorption peak at 2855 cm^{-1} arises due to C-H stretching vibrations. The absorption peaks at 1633, 1286, and 1459 cm^{-1} can be assigned to C=C stretching, C-O stretching, and C-H bending vibrations. The peak at 1113 cm^{-1} was due to the absorption of C-O stretching vibration. The strong absorption band at 443 cm^{-1}, and 714 cm^{-1} were assigned to C-C bending vibrations.

3.5 UV-Visible Absorption Analysis

The MgO/rGO sample's UV-visible absorption spectra (Fig. 8) were captured using a Perkin-Elmer Lambda 35 UV-visible absorption spectrometer. Fig. 9 displays the MgO/rGO nanoparticles that were analyzed between 200 and 1200 nm (267 nm - high absorption peak). At 4.6441 eV, the optical energy band gap was computed. The UV-visible reflectance spectra of MgO/rGO nanoparticles are displayed in Fig. 10. From this data, it was observed that the band gap energy of MgO/rGO was 2.7 times greater than the rGO alone.

The band gap energy was calculated using the equation,

$$E = h\upsilon \quad \ldots (2)$$

$$Eg = hc/\lambda \text{ eV} \quad \ldots (3)$$

where,

h is Plank's constant (6.626×10-34 Js)
c is the speed of light (3×108 ms^{-1})
λ is the wavelength (m)

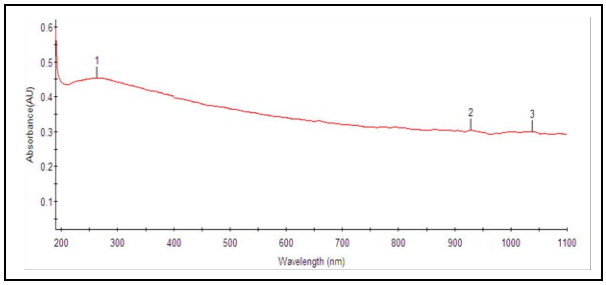

Fig. 8: UV-Visible absorption spectrum of rGO nanoparticles

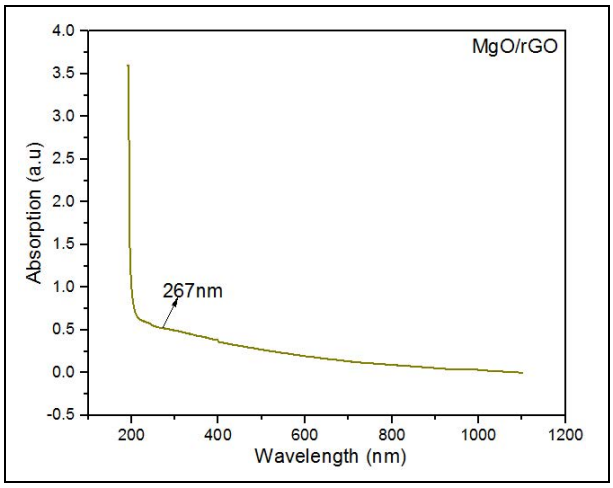

Fig. 9: UV-Visible absorption spectrum of MgO/rGO nanoparticles

3.6 Photoluminescence (PL)

The photoluminescence spectra of MgO/rGO nanoparticles are displayed in Fig. 11. These spectra correspond to several emission bands that are seen at 361, 376, 410, 439, 489, 505, 532, and 535 nm. Between 361 and 376 nm near violet areas were detected. Faint blue band emissions at 489, 505, 523, and 535 nm suggested the presence of weak green band emissions. The shift of MgO/rGO nanoparticles (maxima emission at 361 nm that is in UV region when compared with rGO (maxima emission at 578 nm that is in visible region) (Ding *et al.* 2018) reveals that the MgO/rGO has more capacitance behaviour than rGO alone.

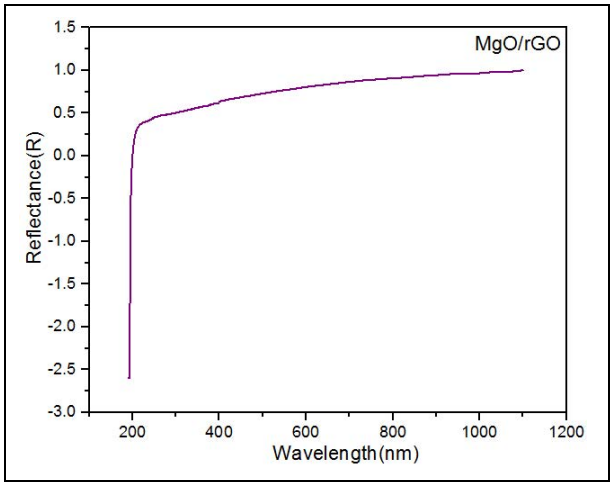

Fig. 10: UV-Visible absorption spectrum of MgO/rGO nanoparticles

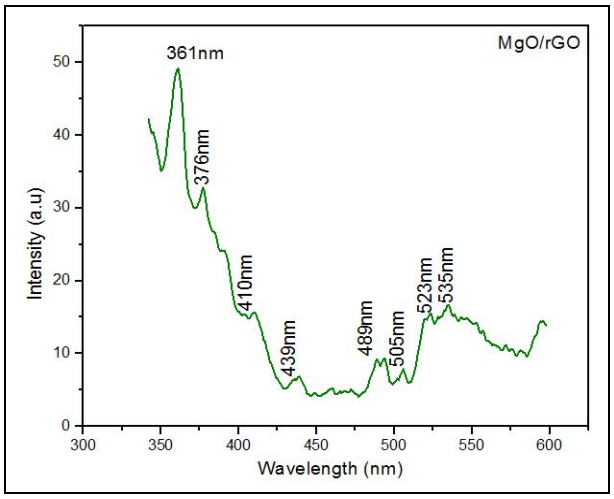

Fig. 11: PL spectrum of MgO/rGO nanoparticles

3.7 Cyclic Voltammetry (CV)

A strong and well-liked electrochemical method frequently used to study the reduction and oxidation processes is cyclic voltammetry (CV). Studying chemical reactions triggered by electron transfer, such as catalysis, is also very beneficial. The applied voltage (V) is represented by the x-axis, while the resultant current (A) passed is represented by the y-axis. Cyclic voltammetry investigations of rGO and MgO/rGO nanoparticles were conducted at a scan rate of 2 mV (Figures 12 and 13). For rGO and MgO/rGO nanoparticles, the specific capacitance values were determined to be 18 F/g and 51 F/g, respectively. The specific capacitance value of MgO/rGO was 2.8 times greater than that of rGO.

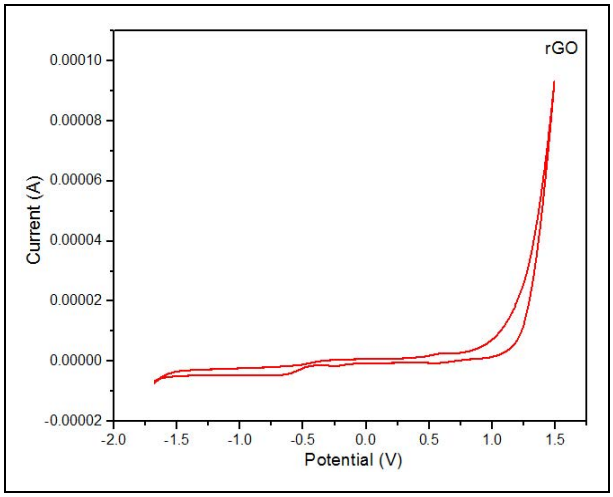

Fig. 12: PL spectrum of MgO/rGO nanoparticles

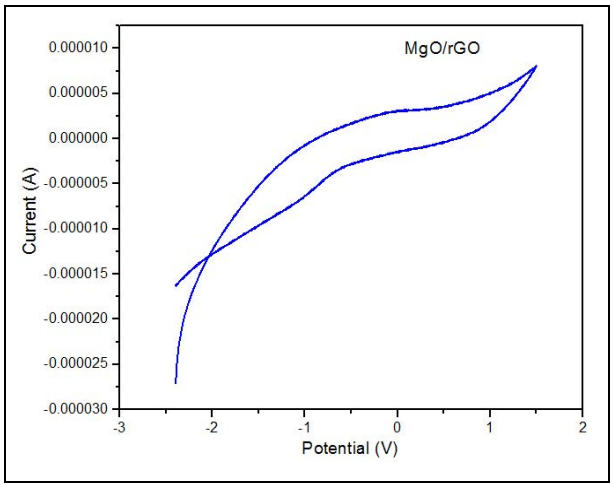

Fig. 13: Cyclic voltammetry analysis of MgO/rGO nanoparticles

4. CONCLUSION

MgO/rGO nanoparticles were successfully synthesized using the co-precipitation technique and rGO was synthesised by ultrasonication techniques. The XRD data were used to calculate the crystallite size, lattice constant, micro-strain, and dislocation density. The HR-TEM evaluation's d-spacing value strongly matched the XRD pattern. Particle size values for MgO/rGO nanoparticles were ranged from 24.053 to 35.364 nm, from TEM images. The crystal's form was found to be

cubic in nature. The EDAX spectrum was used to carry out the elemental analysis. The FTIR spectrum was used to determine the functional group. The UV-Vis absorption spectra were used to calculate the band gap energy. The outcome demonstrated the high optical behaviour, high band gap energy, and high specific capacitance values for MgO/rGO in comparison with rGO alone.

FUNDING

This research received no specific grant from any funding agency in the public, commercial, or not-for-profit sectors.

CONFLICTS OF INTEREST

The authors declare that there is no conflict of interest.

COPYRIGHT

REFERENCES

Abdel-Aal, S. K., Ionov, A., Mozhchil, R. N. and Naqvi, A. H., Simple synthesis of graphene nanocomposites MgO–rGO and Fe2O3–rGO for multifunctional applications, *Appl. Phys. A*, 124(5), 365 (2018). https://doi.org/10.1007/s00339-018-1748-5

Akrami, M., Danesh, S. and Eftekhari, M., Comparative Study on the Removal of Cationic Dyes Using Different Graphene Oxide Forms, *J. Inorg. Organomet. Polym. Mater.*, 29(5), 1785–1797 (2019). https://doi.org/10.1007/s10904-019-01140-0

Bhargava, R. and Khan, S., Effect of reduced graphene oxide (rGO) on structural, optical, and dielectric properties of Mg(OH) 2 /rGO nanocomposites, *Adv. Powder Technol.*, 28(11), 2812–2819 (2017). https://doi.org/10.1016/j.apt.2017.08.008

Ding, J. J., Chen, H. X., Feng, D. Q. and Fu, H. W., Investigation on photoluminescence emission of (reduced) graphene oxide paper, *IOP Conf. Ser. Mater. Sci. Eng.*, 292, 012097 (2018). https://doi.org/10.1088/1757-899X/292/1/012097

Liu, L., Yu, J. and Chen, X., Enhanced Stability and Reusability of Alcohol Dehydrogenase Covalently Immobilized on Magnetic Graphene Oxide Nanocomposites, *J. Nanosci. Nanotechnol.*, 15(2), 1213–1220 (2015). https://doi.org/10.1166/jnn.2015.9024

Saini, A., Kumar, A., Anand, V. K. and Sood, S. C., Synthesis of Graphene Oxide using Modified Hummer's Method and its Reduction using Hydrazine Hydrate, *Int. J. Eng. Trends Technol.*, 40(2), 67–71 (2016). https://doi.org/10.14445/22315381/IJETTV40P21

Sarkar, S. and Mahalingam, V., Tuning the crystalline phase and morphology of the YF3:Eu3+ microcrystals through fluoride source, *CrystEngComm*, 15(29), 5750 (2013). https://doi.org/10.1039/c3ce40554k

Sudesh, K. N., Das, S., Bernhard, C. and Varma, G. D., Effect of graphene oxide doping on superconducting properties of bulk MgB 2, *Supercond. Sci. Technol.*, 26(9), 095008 (2013). https://doi.org/10.1088/0953-2048/26/9/095008

Sun, L., Su, T., Xu, L. and Du, H.-B., Preparation of uniform Si nanoparticles for high-performance Li-ion battery anodes, *Phys. Chem. Chem. Phys.*, 18(3), 1521–1525 (2016). https://doi.org/10.1039/C5CP06585B

Wahab, R., Ahmad, N., Alam, M. and Ansari, A. A., Nanocubic magnesium oxide: Towards hydrazine sensing, *Vacuum*, 155, 682–688 (2018). https://doi.org/10.1016/j.vacuum.2018.06.026

Wang, S., Gao, F., Zhao, Y., Liu, N., Tan, T. and Wang, X., Two-Dimensional CeO2/RGO Composite-Modified Separator for Lithium/Sulfur Batteries, *Nanoscale Res. Lett.*, 13(1), 377 (2018). https://doi.org/10.1186/s11671-018-2798-5

Zhang, L., Yu, X., Hu, H., Li, Y., Wu, M., Wang, Z., Li, G., Sun, Z. and Chen, C., Facile synthesis of iron oxides/reduced graphene oxide composites: application for electromagnetic wave absorption at high temperature, *Sci. Rep.*, 5(1), 9298 (2015). https://doi.org/10.1038/srep09298